AD-A124 143 FATIGUE CRACK PROPAGATION IN AMORPHOUS POLY(ETHYLENE TEREPHTHALATE)(U) LEHIGH UNIV BETHLEHEM PA COXE LAB A RAMIREZ ET AL. DEC 82 TR-13 N00014-77-C-0633 1/1

UNCLASSIFIED F/G 20/11 NL

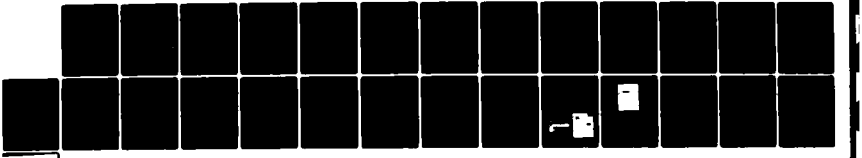

END
DATE FILMED
4-83
DTIC

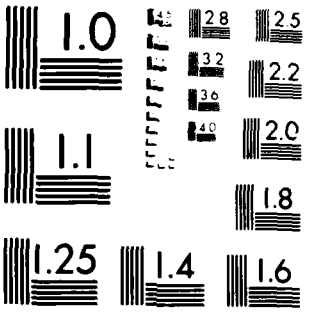

SECURITY CLASSIFICATION OF THIS PAGE (When Data Entered)

REPORT DOCUMENTATION PAGE

READ INSTRUCTIONS BEFORE COMPLETING FORM

1. REPORT NUMBER: Technical Report #13	2. GOVT ACCESSION NO.: AD-A124143
3. RECIPIENT'S CATALOG NUMBER	
4. TITLE (and Subtitle): Fatigue Crack Propagation in Amorphous Poly(ethylene terephthalate)	5. TYPE OF REPORT & PERIOD COVERED: Technical Report
	6. PERFORMING ORG. REPORT NUMBER
7. AUTHOR(s): A. Ramirez, J. A. Manson, and R. W. Hertzberg	8. CONTRACT OR GRANT NUMBER(s): N00014-77-C-0633
9. PERFORMING ORGANIZATION NAME AND ADDRESS: Materials Research Center, Lehigh University, Bethlehem, PA 18015	10. PROGRAM ELEMENT, PROJECT, TASK AREA & WORK UNIT NUMBERS: NR356-670
11. CONTROLLING OFFICE NAME AND ADDRESS: Office of Naval Research, 800 North Quincy Street, Arlington, VA 22217	12. REPORT DATE: December 1981
	13. NUMBER OF PAGES
14. MONITORING AGENCY NAME & ADDRESS (if different from Controlling Office)	15. SECURITY CLASS. (of this report): Unclassified
	15a. DECLASSIFICATION/DOWNGRADING SCHEDULE

16. DISTRIBUTION STATEMENT (of this Report)

This document has been approved for public release; its distribution is unlimited.

17. DISTRIBUTION STATEMENT (of the abstract entered in Block 20, if different from Report)

DTIC ELECTE FEB 7 1983

18. SUPPLEMENTARY NOTES

19. KEY WORDS (Continue on reverse side if necessary and identify by block number)

Poly(ethylene terephthalate)	Fatigue
Glassy Polymers	Fracture
Crystalline Polymers	Mechanisms of Fracture

20. ABSTRACT (Continue on reverse side if necessary and identify by block number)

Earlier studies of fatigue crack propagation (FCP) in polymers have shown a general superiority of crystalline relative to amorphous polymers in terms of FCP resistance. In order to study in detail the effect of crystalline content and character on FCP rates, Poly(ethylene terephthalate) (PET) was selected as a convenient material in which a wide range of crystallinity can be obtained. In order to provide a base-line for comparison, FCP rates were determined for essentially amorphous polymers covering a range of molecular

DD FORM 1 JAN 73 1473 EDITION OF 1 NOV 65 IS OBSOLETE S/N 0102-014-6601 007

SECURITY CLASSIFICATION OF THIS PAGE (When Data Entered)

weight. Surprisingly, the essentially amorphous PET turned out t[illegible] tant to FCP as the best crystalline polymers so far observed. In this paper, several observations about FCP rates and fracture topography are reported: FCP rates agree well with the Paris equation over a wide range of ΔK; in any case, the higher the molecular weight, the greater the crack growth resistance according with the Manson-Hertzberg relationship previously established. Fracture surface analysis revealed evidence of softening and drawing, and extensive plastic and shear deformation. We suggest that PET can undergo both extensive drawing and actual crystallization to form an efficient, crack-resistant network. Thus PET appears to be the first thermoplastic observed to be self-reinforcing in fatigue.

OFFICE OF NAVAL RESEARCH

Contract N00014-77-C-1234

Task No. NR 056-670

TECHNICAL REPORT NO. 13

Fatigue Crack Propagation

in

Amorphous Poly(ethylene terephthalate)

by

Alvaro Ramirez, John A. Manson and Richard W. Hertzberg

Prepared for Publication

in

Polymer Engineering and Science

Materials Research Center
Coxe Laboratory #32
Lehigh University
Bethlehem, PA 18015

December 1982

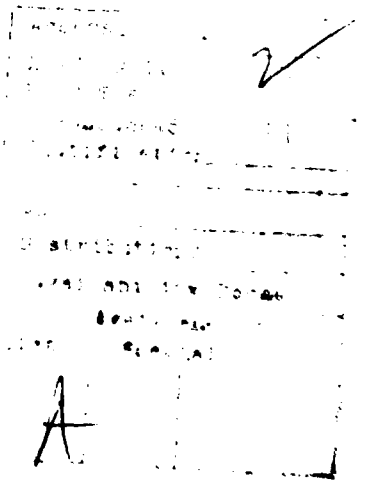

Fatigue Crack Propagation in Amorphous Poly(ethylene terephthalate)

Alvaro Ramirez, John A. Manson and Richard W. Hertzberg
Materials Research Center
Lehigh Univeristy
Bethlehem, PA 18015

Abstract

Earlier studies of fatigue crack propagation (FCP) in polymers have shown a general superiority of crystalline relative to amorphous polymers in terms of FCP resistance. In order to study in detail the effect of crystalline content and character on FCP rates, Poly(ethylene terephthalate) (PET) was selected as a convenient material in which a wide range of crystallinity can be obtained. To provide a base-line for comparison, FCP rates were determined for essentially amorphous polymers covering a range of molecular weight. Surprisingly, the essentially amorphous PET turned out to be as resistant to FCP as the best crystalline polymers so far observed. In this paper, several observations about FCP rates and fracture topography are reported: FCP rates agree well with the Paris equation over a wide rnage of ΔK; in any case, the higher the molecular weight, the greater the crack growth resistance according with the Manson-Hertzberg relationship previously established. Fracture surface analysis revealed evidence of softening and drawing, and extensive plastic deformation. We suggest that PET can undergo, under cycling loading, both extensive drawing and actual crystallization at the crack tip to form an efficient, crack-resistant network. Thus PET appears to be the first thermoplastic observed to be self-reinforcing in fatigue.

Introduction

In our earliest studies of fatigue crack propagation (FCP) in polymers (1), we observed that the range of behavior exhibited was much greater than is the case with metals. Thus in a typical poly(methyl methacrylate) PMMA a crack grew 1300X faster than in a typical polycarbonate, at an equivalent range in stress intensity factor, ΔK. Since a specimen of nylon 66 was found to be still more resistant than the polycarbonates it was suggested that in comparison with an amorphous polymer, a crystalline polymer might well provide mechanisms for dissipating energy that do not exist in an amorphous polymer. In other words, extensive transformation of a crystalline network to a new morphology takes place on deformation past the yield point (2,3). Such a transformation is accompanied by the expenditure of considerable energy in addition to that corresponding to the surface energy. More recent experiments have confirmed the general superiority of crystalline relative to amorphous polymers in terms of FCP resistance (1). To be sure, significant increases in FCP resistance in amorphous or mesomorphic polymers like PMMA and PVC can be achieved simply by increasing the molecular weight [and hence the effectiveness of the entanglement network opposing progress of the crack] or by including a rubbery phase [thereby enhancing the ductility of the matrix] (4,5). However, while some of these materials were as resistant to FCP as polycarbonate, none achieved the resistance of nylon 66 (6), nylon 6 (6), polyacetal (7), or, especially, poly(vinylidene fluoride) (8) — all crystalline polymers. One amorphous polyamide was also studied, and found to be much less resistant to FCP than polycarbonate (1, p. 130).

In view of these findings, it was decided to study the effects of crystalline content and character on FCP rates (9). In fact, Laghouati et al.

(10) have found crystalline texture in polyethylene to play a major role in FCP resistance. Unfortunately, a wide range of crystallinity cannot be obtained in either polyethylene or nylon 66, at least with specimens thick enough to study FCP rates. We therefore sought a polymer in which the crystallinity could be readily varied from essentially zero to a reasonbly high value (say, 40%). Poly(ethylene terephthalate) (PET) was selected as a candidate having that advantage; in addition, it was possible to obtain a range of molecular weights. While PET has been most commonly used as a fiber or as a biaxially oriented sheet, blow-molded products are being used to an increasing extent, and there has been considerable interest in injection molding as well (11).

In order to provide a base-line for comparison, FCP rates were determined for essentially amorphous PET's covering a range of molecular weight. Surprisingly, the essentially amorphous polymers turned out to encompass about as high a range of FCP resistance observed in <u>any</u> polymer so far — amorphous <u>or</u> crystalline. In this paper, preliminary observations of FCP rates and fracture topography are reported, and future explorations suggested.

Experimental

Characterization

Injection-molded sheets of PET (3mm x 15cm x 15cm) were kindly supplied by Dr. S. L. Kim throguh the courtesy of the Goodyear Tire and Rubber Co. The sheets had been quenched to a room temperature of 25°C in order to produce an essentially amorphous product. Number-average molecular weights, $\bar{M}_n$, were determined viscometrically in 60/40 phenol/tetrachloroethane solutions at 25°C using the equation $[\eta] = 7.5 \times 10^{-4} \bar{M}_n 0.68$ (12).

Values of M_w/M_n, the ratio of weight to number-average molecular weight, were estimated from the relationship $M_w/M_n = 1+p$, where $M_n=M_o/(1-p)$, p being the fractional conversion, and M_o the molecular weight of the repeat unit (13). Since PET is well known to undergo degradation of molecular weight on heating, molecular weights were determined before fatigue testing.

The degree of crystallinity was determined using a Perkin-Elmer differential scanning calorimeter, model DSC-1B, a reference value for the heat of fusion of 28.1 cal/g (117 J/g) (14), and a scanning rate of 40°C/min. To effect this estimation, the area for the exothermic peak between 408 and 470°K [which occurs due to crystallization during the DSC scan] was subtracted from the area of the endothermic peak between 506 and 530°K [which corresponds to the melting of the crystallites formed during the scan]. For comparison, a sample of PET-D was crystallized to the extent of 27% by heating to 120°C for 3 hr. Fig. 1 shows typical scans for the nominally amorphous PET as well as for crystallized materials. To examine changes in the state of the polymer due to the fatigue process in the plastic zone, several thin sections of polymer were cut from all the crack surfaces and from the strongly whitened zone prior to failure, and scanned at 40°C/min for evidence of crystallinity. The sections were thin enough (<0.5 mm) to exclude sampling of the bulk material, which is unaffected during the fatigue process; thus the sections are representative of the diffuse whitened zone under the crack plane (see Morphology). Crystallinities were also determined for amorphous and fully crystalline PET, respectively (14). Values of T_g were obtained with the DSC, at a scanning rate of 10°C/min. Before testing, specimens were examined visually between crossed polaroids to check for birefringence (none found), and stored in a dry box until use.

Fatigue tests were performed in air on notched compact-tension specimens (3.2 mm x 7.5 cm x 7.5 cm) at a sinusoidal frequency of 10 Hz, and a ratio of minimum to maximum load of 0.1, using an electrohydraulic closed-loop test machine and standard procedures (4). Values of the stress intensity factor range, ΔK, were calculated from the equation $\Delta K = Y\Delta\sigma\sqrt{a}$, where Y is a geometrical factor, $\Delta\sigma$ the stress load and $\underline{a}$ the crack length (15). FCP rates were plotted in terms of the crack growth rate per cycle, da/dN, as a funtion of ΔK. ΔK_{max} was taken to be the final value of ΔK prior to uncontrolled crack growth, and a relative value of fracture toughness, K_c, was taken as equal to $\Delta K_{max}/0.9$ (4). Fracture surfaces were examined using an optical microscope (reflected light) and an ETEC scanning electron (SEM), for which specimens were prepared by gold/palladium coating. Fracture surfaces and portions of the face of the specimen containing the crack were also etched (for 20 hr) using a 40% solution of methylamine in water to reveal morphological detail; this etchant preferentially attacks amorphous polymer (16). Preliminary measurements of temperatures at the crack tip were made using a Barnes infrared camera, model RM-2B.

Results and Discussion

Characterization

As shown in Table 1, the PET specimens range in $\bar{M}_n$ from 12,500 to 28,700. As expected, the values of $\bar{M}_n$ are all lower than those obtained before molding (see Fig. 2). Since FCP rates are sensitive to molecular weight, it is important to characterize $\bar{M}_n$ after the application of any thermal treatment. The essentially amorphous nature of the quenched samples was confirmed by use of the DSC (Fig. 1) and the density gradient column. Values of T_g are self-consistent, and in agreement with those in the

literature (17). Thus although dynamic-mechanical tests are yet to be made, the specimens appear so far to be well-behaved in all respects.

Fatigue Crack Propagation

As shown in Fig. 3, all the curves of FCP as a function of ΔK agree well with the Paris equation over a wide range of ΔK: $da/dN=A\Delta K^n$. [For values of n see Table 1]. With this range of ΔK, duplicate tests gave values of da/dN (at a given ΔK) that agreed within ±15%. Average slopes of the da/dN curve (Table 2) tend to increase from a value of 5.8 (±0.8) to 8.8 (±0.7) as the value of $\bar{M}_n$ increases from 12,500 to 28,700. The last points on the curves correspond to the last observations prior to the onset of a stage of uncontrolled crack growth, which lasted for from 15 to 20 cycles. Then the amorphous samples failed by gross yielding without separation into two pieces, while the crystalline sample failed by yielding accompanied by actual rupture. In all cases, crack growth was accompanied by a progressive increase of surface temperature at the crack tip. Preliminary observations with PET-A indicate that the temperature rises after cycling begins to 29°C, remains at 29°C until just before final yielding, when the temperature rises rapidly to 80-90°C. PET-D behaves similarly, except that the steady-state temperature is slightly higher, 33°C. (A detailed study of temperature profiles at crack tips as a function of loading conditions is in progress.)

The tendency of the FCP curves to converge at high values of ΔK would be expected to result in a fairly small range in ΔK_{max}. In fact values of ΔK_{max} range between 5.0 and 6.3 $MPa\sqrt{m}$ for the amorphous polymers, in comparison with a value of 6.8 $MPa\sqrt{m}$ for the 27%-crystalline PET-D. While ΔK_{max} increases as $\bar{M}_n$ increases from 12,500 to 19,500, a further increase in $\bar{M}_n$ has no significant effect on ΔK_{max}. Such an effect has been noted before with

polyacetal (18) and polycarbonate (PC) (19) at room temperature. On the other hand, the slopes for poly(vinyl chloride) (5), poly(methyl methacrylate (4), nylon 66 (6), and PC [at -30°C (19)] are essentially constant, while the curves diverge in the case of high-density PE (10). The significance of the slope behavior clearly requires further investigation.

In any case, clearly the higher the molecular weight, the greater the resistance to crack growth (especially at lower values of ΔK) — an observation made previously by ourselves and others (1). Indeed, as shown in Fig. 4, the relationship of Eq. 1 holds quite well, as it does for PVC and PMMA (4,5):

$$\frac{da}{dN} = A' \, e^{B/M} \, \Delta K^n \qquad (1)$$

While discovered empirically (4), a relationship of this form can be derived based on the assumption that FCP ressistance is controlled generally by the effectiveness of molecular entanglement networks, and in particular, by the fraction of molecules possessing values of M greater than the critical value required for formation of an effective entanglement network (20).

It is also interesting to relate the force required to drive a fatigue crack at a constant speed to the quasi-static fracture toughness. Thus it has been shown that ΔK^*, the value of ΔK required to drive a crack at constant speed, is a linear function of K'_c for many polymers (1, ch.3), illustrating a basic correlation between fatigue and static response. It is true that K'_c as defined herein for amorphous PET (which fails by gross yielding) certainly does not reflect a true fracture toughness in the sense of a critical value of K required for actual fracture. Nevertheless, the values of ΔK^* as a function of K'_c do fall within the range exhibited by all other

polymers studied (Fig. 5). Thus in a general way, the ability of PET to withstand high loads without tearing apart at the end of the test is reflected in a very high driving force to attain a given value of da/dN.

Indeed a comparison of PET with all other polymers studied to date (Fig. 6), shows that amorphous PET's exhibit FCP rates at a given value of ΔK that are lower than for other polymers, with the exception of the partially crystalline 27 PET-D. Hence, although values of ΔK_{max} are not as high as for some other polymers, amorphous PET exhibits a remarkable resistance to fatigue crack growth.

Of course, specimen thickness may play a major role with such a ductile polymer. For example, with PC (21), 3 mm-thick specimens were seen to be much more resistant to FCP than 6-mm-thick specimens; at a ΔK of $2MPa\sqrt{m}^{-1/2}$, da/dN varied from $4x10^{-3}$ to $3x10^{-4}$ mm/cycle as the thickness was changed from 6 to 3 mm, respectively (a ratio of ~13/1). Generally similar results were also noted by Pitman and Ward (19). Clearly the effect of thickness needs to be established, though it is not yet certain whether or not adequate through-thickness quenching can be obtained with specimens thicker than 3 mm. In any case, even if a thickness effect similar to that in PC is operative, amorphous PET behaves better than PC (having about the same molecular weight) with respect to the resistance to fatigue crack propagation.

Preliminary examination of the fracture surfaces of all four amorphous samples revealed (Figs. 7 and 8) a complex and unusual combination of features not reported before in amorphous polymers (1, ch. 4). After a region of stable crack growth (comprising zones A and B), a region of uncontrolled crack growth with fracture markings, zone C, is evident (as mentioned above).

Considerable whitening was evident in zone C, as well as significant pull-in from the edges. Zone D corresponds to the ligament remaining when the compliance exceeded the capability of the instrument. Interestingly, no discontinuous growth bands were observed (1, ch. 4); the markings seen in zone C correspond to single load cycles. When viewed from the side, all specimens exhibited a birefringent diffuse whitened zone under the crack plane; the thickness of this zone increased with increasing ΔK, reaching a value of $\sim$3 mm just prior to the beginning of zone C, and continuing to grow thereafter (Fig. 9). Optical microscope and SEM observations on fresh and etched samples revealed the presence of fissures in the whitened zone, running parallel to the main crack and believed to be crazes. (A more detailed study of the morphology is in progress.)

In general, there was much evidence of softening and drawing, especially in zone A. Interestingly, zone A, which exhibited a honeycomb structure, resembled the surface of fatigue-cracked low-density polyethylene (22), in which failure appeared to occur by the growth and coalescence of microvoids The surface of zone B was birefringent, and was characterized by large ($\sim$150-600μ) parabolic features. All parabolae included small ball-like features, sometimes at the foci and sometimes not.

Interestingly, the total width of zone A whose surface was <u>not</u> birefringent was seen to vary in proportion to ΔK^2, as has been noted for shear lips in polycarbonate (PC) (19). While zone A does not appear to resemble clear-cut shear lips as seen in PC, evidently the phenomenon involved in the formation of zone B may well reflect a shear process associated with plane-stress conditions. Thus the stress conditions appear to comprise a combination of plane strain with plane stress. If we assume that a plane-stress

component is present, the width of zone B, r_y, may be related (1,p.148) to K and the yield stress, σ_y:

$$r_y = \frac{1}{2\pi} \frac{K^2}{\sigma_y^2} \qquad (2)$$

Using equation 2, calculated values of σ_y were found to fall between 61 and 54 MPa, as ΔK was increased from 2.3 to 3.8 $MPa \cdot m^{1/2}$. These values may be compared with a typical value of 82 MPa reported in the literature (17). Since temperatures at the crack tip undoubtedly significantly exceed those at the specimen faces, the values of σ_y may well be reasonable.

Mechanisms of Toughening

As mentioned above, amorphous PET exhibits very extensive plastic deformation during fatigue crack growth, in this respect resembling PC (1, ch.4), rubber-toughened PVC (23) and low-density polyethylene (22). The absence of discontinuous crack growth (i.e., development of a craze ahead of the crack tip with a lifetime extending over many cycles) is consistent with the diffuse zone of damage actually observed (1, ch. 4). The high level of shear deformation in plane stress is surely in part associated with the thinness of the specimens in part responsible for the exceptional FCP resistance observed. Nevertheless, the development of crystallinity at the crack tip during the test must surely play a role. As shown in Fig. 10, the % crystallinity increases in a regular manner with increasing crack length (and hence with ΔK^2). Morphology may also play a role, for a specimen crystallized to a level of 2-10% exhibits a lower FCP rate than amorphous PET when its crack-tip crystallinity is also 2-10% (24); in fact, the morphology induced by annealing above the T_g is known to be different from that produced by strain-crystallization (25). In any case, crystallization during the test may be expected to have two beneficial effects: the development of a network whose disruption requires the

expenditure of much energy, and provision of a general heat sink that reduces the amount of energy available for crack extension. While such a mechanism has been proposed by Andrews to explain the resistance to FCP in strain-crystallizing elastomers (26), PET appears to be the first thermoplastic observed to be self-reinforcing in fatigue crack propagation.

Conclusions

The following observations and conclusions may be stated:

1. Nominally amorphous PET exhibits an exceptionally high resistance to fatigue crack propagation.

2. While part of the resistance may be ascribed to the development of a significant component of plane stress behavior, the development of crystallinity at the crack tip during the test must surely play a major role in toughening, both by generating a strong and tough network ahead of the crack and by providing a harmless mode for dissipating strain energy that would otherwise be available for crack extension.

Acknowledgements

The authors acknowledge partial support from the Polymers Program, National Science Foundation, Grant No. DMR77-10063, and by the Office of Naval Research. The efforts of our former colleague, Dr. S. L. Kim, Goodyear Tire and Rubber Co., are very much appreciated, as is that company's donation of the samples.

References

1. R. W. Hertzberg and J. A. Manson, "Fatigue in Engineering Plastics," Academic Press, New York, 1980, ch. 3.

2. G. Meinel and A. Peterlin, J. Polym. Sci. Polym. Lett. Ed. 9, 67 (1971).

3. R. S. Samuels, "Structured Polymer Properties," Wiley, New York, 1974.

4. S. L. Kim, M. D. Skibo, J. A. Manson and R. W. Hertzberg, Polym. Eng. Sci. 17, 1974 (1977)

5. C. Rimnac, S. M. Webler, J. A. Manson, and R. W. Hertzberg, J. Macromol. Sci. Phys.,

6. P. E. Bretz, R. W. Hertzberg, and J. A. Manson, J. Mater. Sci.

7. R. W. Hertzberg and J. A.Manson, "Fatigue in Engineering Plastics," Academic Press, New York, 1980, ch. 3, p. 116.

8. R. W. Hertzberg, J. A. Manson, and M. D. Skibo, J. Mater. Sci., 15, 252 (1975).

9. ONR Project N00014-77-C-0633, Lehigh University.

10. F. X. deCharentenay, F. Laghouati, and J. Dewas, in "Deformation, Yield and Fracture of Polymers," Plastics and Rubber Institute, London, 1979, p. 610.

11. B. W. Pengilly, in "Modern Plastics Encyclopedia," McGraw-Hill, New York, 1980-81, p. 56.

12. L. D. Moore, Proc. ACS meeting, Cleveland, 1, 234 (1960).

13. G. Odian, "Principles of Polymerization," McGraw-Hill, New York, 1970.

14. J. Brandrup and E. H. Immergut, eds., "Polymer Handbook," 2nd ed. Wiley, New York, 1975.

15. W. F. Brown, Jr. and J. E. Srawley, ASTM, STP 410, 142 (1966).

16. G. E. Sweet and J. P. Bell, J. Polym. Sci. Polym. Phys. Ed., 16 1935 (1978).

17. J. A. Brydson, "Plastics Materials," 3rd ed., Butterworth & Co., London, 1975, ch. 25.

18. M. D. Skibo, R. W. Hertzberg, and J. A. Manson, unpublished work, Lehigh University.

19. G. Pitman and I. Ward, Polymer 15, 635 (1980).

20. J. Michel, J. A. Manson, R. W. Hertzberg, this issue.

21. J. A. Manson and R. W. Hertzberg, CRC Crit. Rev. Macromol. Sci. 1(4) 433 (1973).

22. P. E. Bretz, R. W. Hertzberg, and J. A. Manson, in press.

23. M. D. Skibo, S. M. Webler, J. A. Manson, R. W. Hertzberg, and G. A. Collins, ACS Symp. Ser. 95, 311 (1979).

24. A. Ramirez, Ph.D. dissertation in progress, Lehigh University, 1981.

25. G. SY. Yeh and P. H. Geil, J. Macromol. Sci. (Phys.), B1(2), 235 (1967) ibid., B1(2), 251 (1967).

26. E. H. Andrews, J. Appl. Phys. 32 542 (1961).

Table 1. Characteristics of PET Specimens.

Sample	$\bar{M}_n$	$M_w/\bar{M}_n$	Density, g/cm^3	T_g, °C	% Cryst.[a]
PET-A	12,500	1.98	1.334	66[c]	<1(0.8)
PET-B	19,500	1.99	1.334	67[c]	<2(0.8)
PET-C	21,000	1.99	1.333	67[c]	<2(0)
PET-D	28,700	1.99	1.334	67[c]	<2(0.8)
PET-D(27)					27
PET X (A,B,C,D)[b]					(38-46)

[a] Numbers refer to use of DSC and, in parentheses, to use of the density gradient column, respectively.

[b] Samples taken from whitened zones of specimens A to D, inclusive; values of % crystallinity fall within the range given. The melting peak extended from 510 to 560°K (237 to 281°C). For crystallinity in other zones, see Mechanisms of Toughening.

[c] Literature values (17) in the range 66-80°C.

Table 2. Fatigue Characteristics of PET

	$A^a \times 10^7$		K_{max}		$Slope^a, n$	
PET-A	10	1.27	5.0	6.0	5.0	6.6
PET-B	2.57	0.92	5.7	6.4	5.5	6.4
PET-C	0.1	0.25	6.3	5.6	8.0	7.2
PET-D	0.01	0.07	5.5	6.2	9.5	8.1
PET-D(27)					8.5	

[a] From Paris equation, $da/dN = A\Delta K^n$

List of Figures

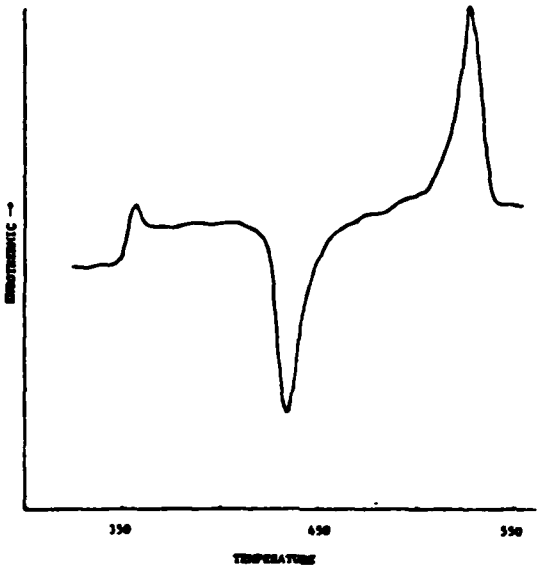

(a)

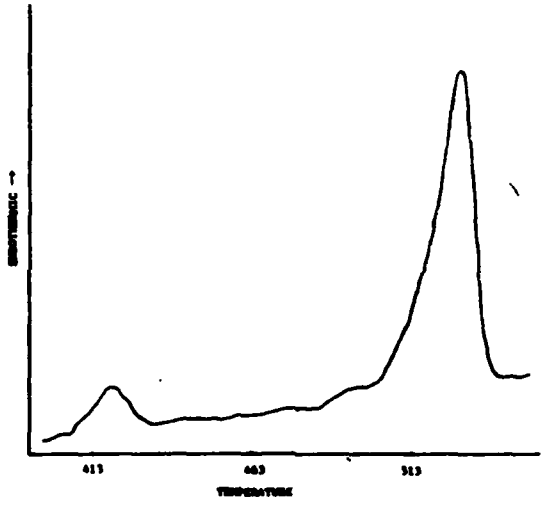

(b)

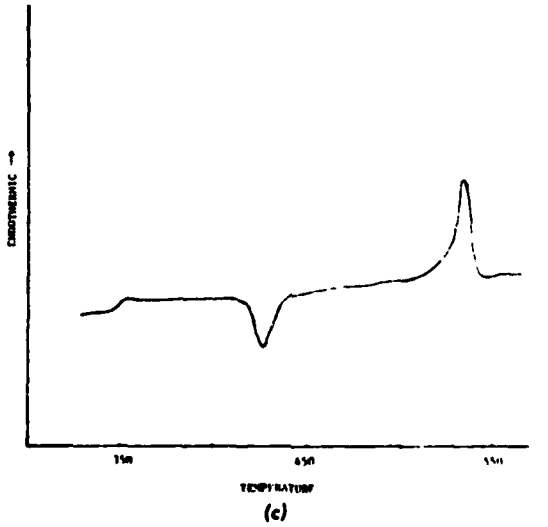

(c)

Fig. 1

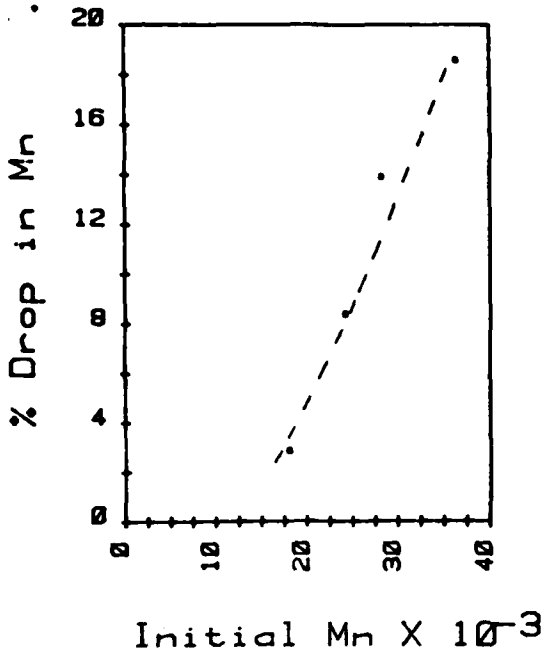

Fig.2

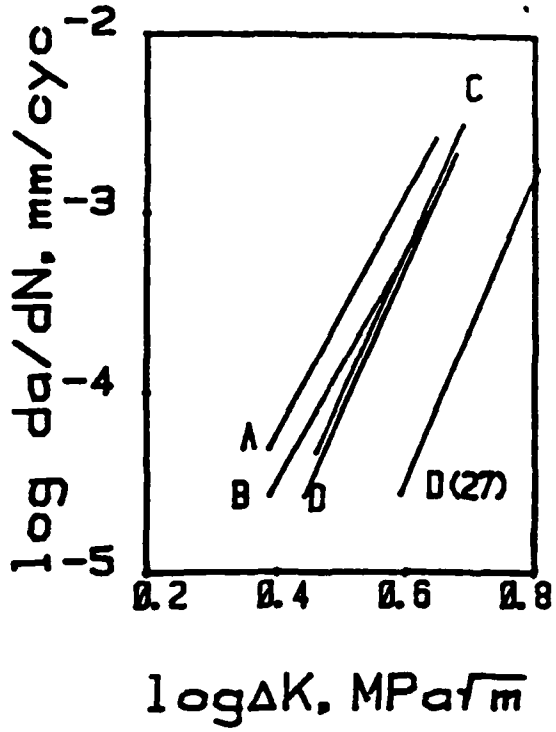

Fig.3

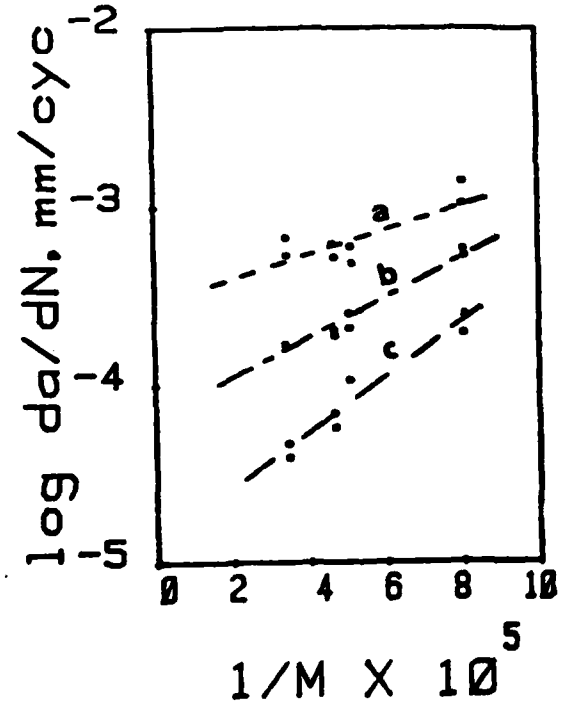

Fig.4

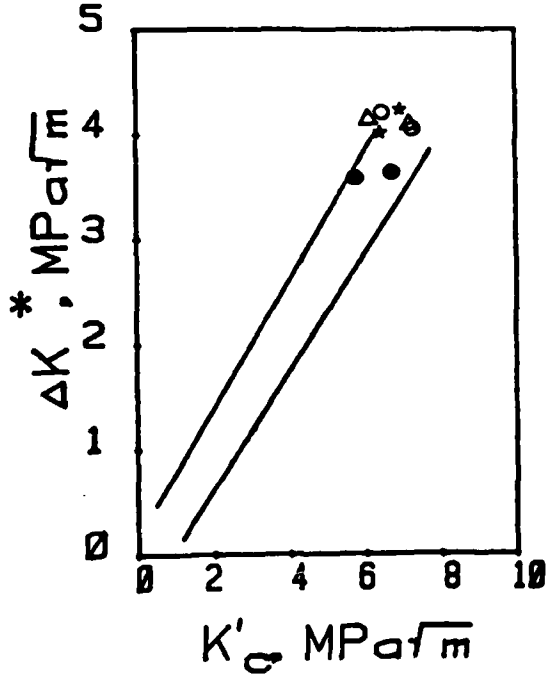

Fig.5

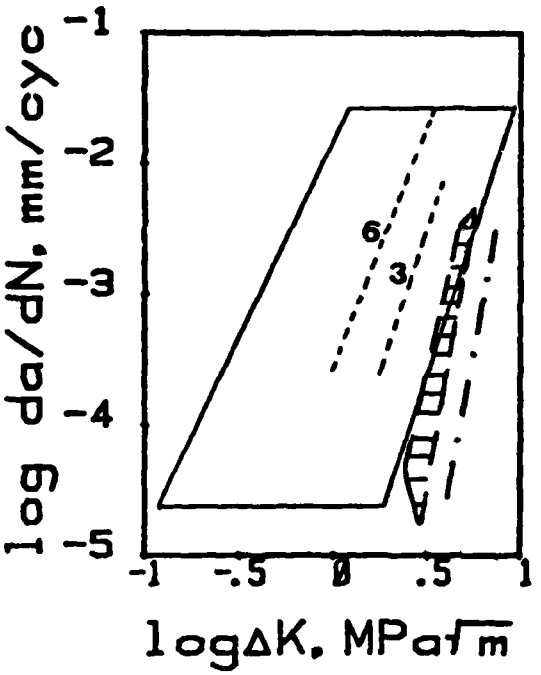

Fig. 6

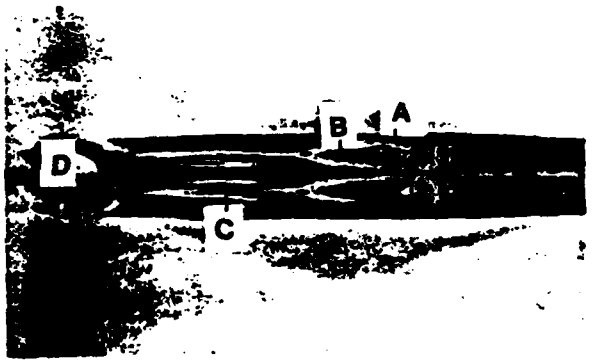

Fig. 7

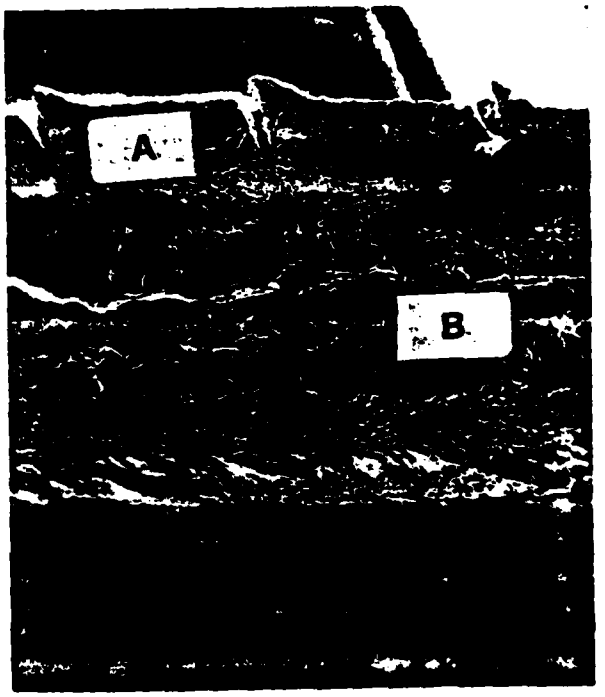

Fig. 8

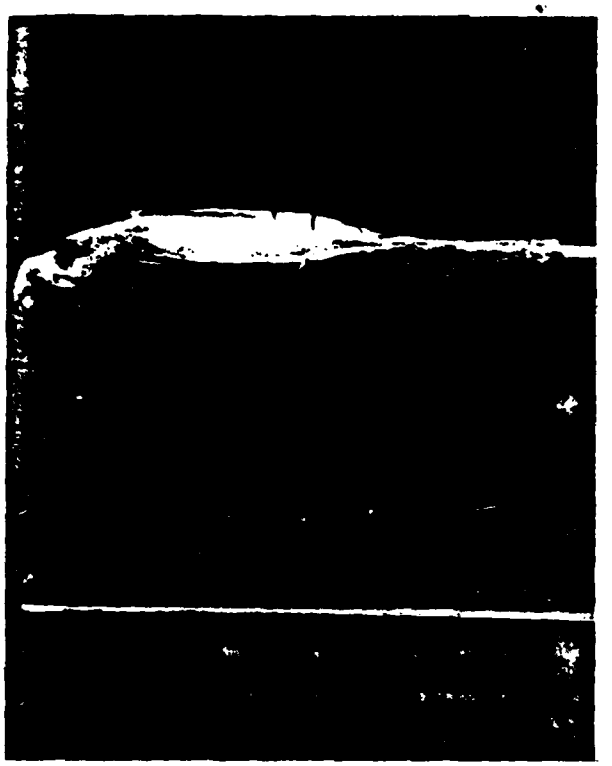

Fig. 9

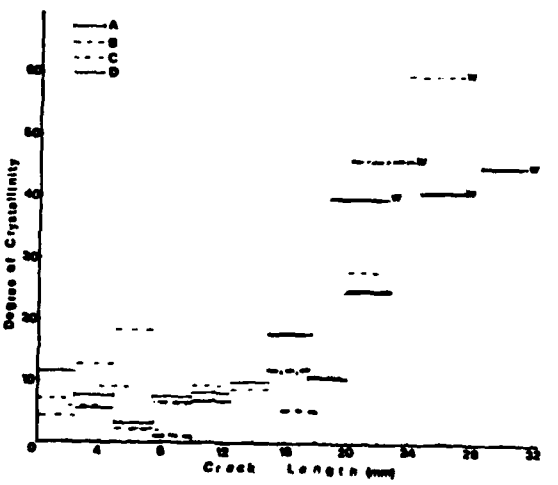
A
B
C
D
Degree of Crystallinity
0
4
8
12
16
20
24
28
32
Crack Length (mm)

Fig. 10

472:GAN:716-4
94/GEN

TECHNICAL REPORT DISTRIBUTION LIST, GEN

	No. Copies
Office of Naval Research Attn: Code 413 800 North Quincy Street Arlington, Virginia 22217	2
ONR Pasadena Detachment Attn: Dr. R. J. Marcus 1030 East Green Street Pasadena, California 91106	1
Commander, Naval Air Systems Command Attn: Code 310C (H. Rosenwasser) Department of the Navy Washington, D.C. 20360	1
Defense Technical Information Center Building 5, Cameron Station Alexandria, Virginia 22314	12
Dr. Fred Saalfeld Chemistry Division, Code 6100 Naval Research Laboratory Washington, D.C. 20375	1
U.S. Army Research Office Attn: CRD-AA-IP P. O. Box 12211 Research Triangle Park, N.C. 27709	1
Mr. Vincent Schaper DTNSRDC Code 2803 Annapolis, Maryland 21402	1
Naval Ocean Systems Center Attn: Dr. S. Yamamoto Marine Sciences Division San Diego, California 91232	1
Naval Ocean Systems Center Attn: Mr. Joe McCartney San Diego, California 92152	1
Naval Weapons Center Attn: Dr. A. B. Amster, Chemistry Division China Lake, California 93555	1
Naval Civil Engineering Laboratory Attn: Dr. R. W. Drisko Port Hueneme, California 93401	1
Dean William Tolles Naval Postgraduate School Monterey, California 93940	1
Scientific Advisor Commandant of the Marine Corps (Code RD-1) Washington, D.C. 20380	1
Naval Ship Research and Development Center Attn: Dr. G. Bosmajian, Applied Chemistry Division Annapolis, Maryland 21401	1
Mr. John Boyle Materials Branch Naval Ship Engineering Center Philadelphia, Pennsylvania 19112	1
Mr. A. M. Anzalone Administrative Librarian PLASTEC/ARRADCOM Bldg 3401 Dover, New Jersey 07801	1

9/82

TECHNICAL REPORT DISTRIBUTION LIST, 356A

	No. Copies
Dr. M. Broadhurst Bulk Properties Section National Bureau of Standards U. S. Department of Commerce Washington, D.C. 20234	2
Naval Surface Weapons Center Attn: Dr. J. M. Augl, Dr. B. Hartman White Oak Silver Spring, Maryland 20910	1
Dr. G. Goodman Globe Union Incorporated 5757 North Green Bay Avenue Milwaukee, Wisconsin 53201	1
Professor Hatsuo Ishida Department of Macromolecular Science Case-Western Reserve University Cleveland, Ohio 44106	1
Dr. David Soong Department of Chemical Engineering University of California Berkeley, California 94720	
Dr. Curtis W. Frank Department of Chemical Engineering Stanford University Stanford, California 94035	
Picatinny Arsenal Attn: A. M. Anzalone, Building 3401 SMUPA-FR-M-D Dover, New Jersey 07801	1
Dr. J. K. Gillham Department of Chemistry Princeton University Princeton, New Jersey 08540	1
Dr. E. Baer Department of Macromolecular Science Case Western Reserve University Cleveland, Ohio 44106	1
Dr. K. D. Pae Department of Mechanics and Materials Science Rutgers University New Brunswick, New Jersey 08903	1
NASA-Lewis Research Center Attn: Dr. T. T. Serofini, MS-49-1 2100 Brookpark Road Cleveland, Ohio 44135	1
Dr. Charles H. Sherman Code TD 121 Naval Underwater Systems Center New London, Connecticut 06320	1
Dr. William Risen Department of Chemistry Brown University Providence, Rhode Island 02191	1
Mr. Robert W. Jones Advanced Projects Manager Hughes Aircraft Company Mail Station D 132 Culver City, California 90230	1
Dr. C. Giori IIT Research Institute 10 West 35 Street Chicago, Illinois 60616	
Dr. R. S. Roe Department of Materials Science and Metallurgical Engineering University of Cincinnatti Cincinnati, Ohio 45221	1
Dr. Robert E. Cohen Chemical Engineering Department Massachusetts Institute of Technology Cambridge, Massachusetts 02139	1
Dr. T. P. Conlon, Jr., Code 3622 Sandia Laboratories Sandia Corporation Albuquerque, New Mexico	1

472:GAN:716-4
94/356A-B

TECHNICAL REPORT DISTRIBUTION LIST, 356A

	No. Copies
Dr. Martin Kaufman Code 38506 Naval Weapons Center China Lake, California 93555	1
Professor S. Senturia Department of Electrical Engineering Massachusetts Institute of Technology Cambridge, Massachusetts 02139	1
Dr. T. J. Reinhart, Jr., Chief Composite and Fibrous Materials Branch Nonmetallic Materials Division Department of the Air Force Air Force Materials Laboratory (AFSC) Wright-Patterson AFB, Ohio 45433	1
Dr. J. Lando Department of Macromolecular Science Case Western Reserve University Cleveland, Ohio 44106	1
Dr. J. White Chemical and Metallurgical Engineering University of Tennessee Knoxville, Tennessee 37916	1
Dr. J. A. Manson Materials Research Center Lehigh University Bethlehem, Pennsylvania 18015	1
Dr. R. F. Helmreich Contract RD&E Dow Chemical Co. Midland, Michigan 48640	1
Dr. R. S. Porter Department of Polymer Science and Engineering University of Massachusetts Amherst, Massachusetts 01002	1
Professor Garth Wilkes Department of Chemical Engineering Virginia Polytechnic Institute and State University Blacksburg, Virginia 24061	1
Professor C. S. Paik Sung Department of Materials Sciences and Engineering Room 8-109 Massachusetts Institute of Technology Cambridge, Massachusetts 02139	1
Professor Brian Newman Department of Mechanics and Materials Science Rutgers, The State University Piscataway, New Jersey 08854	1
Dr. John Lundberg School of Textile Engineering Georgia Institute of Technology Atlanta, Georgia 30332	1


DATE
ILME